Lecture 26

Radiation Fields

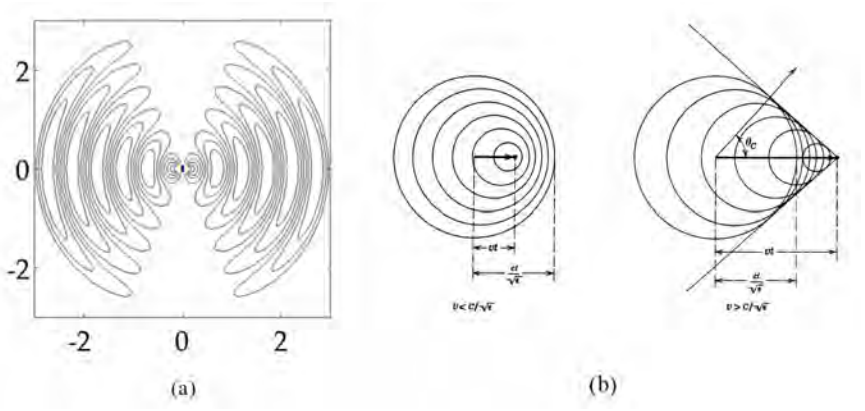

Figure 26.1: (a) Electric field around a time-oscillating dipole (courtesy of physics stack exchange). (b) Equi-potential lines aroud a moving charge that gives rise Cherenkov radiation (courtesy of J.D. Jackson [48]). We will not study Cherenkov (Cerenkov) radiation in this course, but it is written up in [48] and [32]. Its was a Nobel Prize winning discovery.

The reason why charges radiate is because they move or accelerate. In the case of a dipole antenna, the charges move back and forth between poles of the antenna. Near to the dipole source, quasi-static physics prevails, and the field resembles that of a static dipole. If the dipole is flipping sign constantly due to the change in the direction of the current flow, the field would also have to flip sign constantly. But electromagnetic wave travels with a finite velocity. The field from the source ultimately cannot keep up with the sign change of the source field: it has to be 'torn' away from the source field and radiate. Another interesting radiation is the Cherenkov radiation. It is due to a charge moving faster than the velocity of light. As an electron cannot move faster than the speed of light in a vacuum, this can only

happen in the material media or plasma, where the velocity of the electron can be faster than the group velocity of wave in the medium. Ultimately, the electric field from the particle is 'torn' off from the charge and radiate. These two kinds of radiation are shown in the Figure 26.1.

We have shown how to connect the vector and scalar potentials to the sources $\mathbf{J}$ and ϱ of an electromagnetic system. This is a very important connection: it implies that once we know the sources, we know how to find the fields. But the relation between the fields and the sources are in general rather complex. In this lecture, we will simplify this relation by making a radiation field or far-field approximation by assuming that the point where the field is observed is very far from the source location in terms of wavelegth. This approximation is very useful for understanding the physics of the radiation field from a source such as an antenna. It is also important for understanding the far field of an optical system. As shall be shown, this radiation field carries the energy generated by the sources to infinity.

26.1 Radiation Fields or Far-Field Approximation

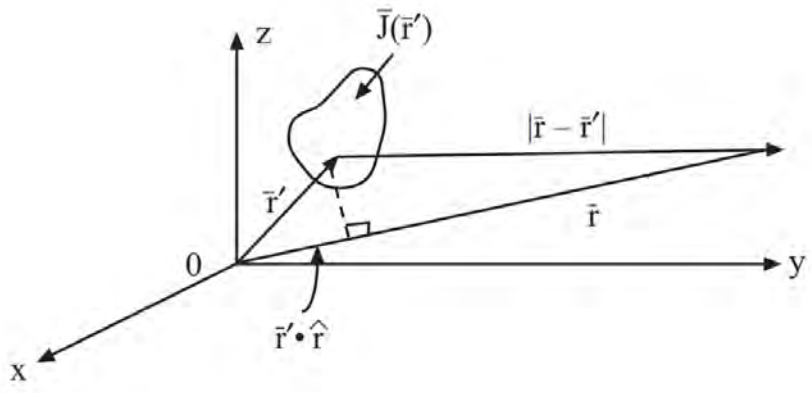

Figure 26.2: The relation of the observation point located a $\mathbf{r}$ to the source location at $\mathbf{r}'$. The distance of the observation point $\mathbf{r}$ to the source location $\mathbf{r}'$ is $|\mathbf{r}-\mathbf{r}'|$.

In the previous lecture, we have derived the relation of the vector and scalar potentials to the sources $\mathbf{J}$ and ϱ as shown in (23.2.29) and (23.2.30)[1] They are given by

$$\mathbf{A}(\mathbf{r}) = \mu \iiint_V d\mathbf{r}' \mathbf{J}(\mathbf{r}') \frac{e^{-j\beta|\mathbf{r}-\mathbf{r}'|}}{4\pi|\mathbf{r}-\mathbf{r}'|} \tag{26.1.1}$$

$$\Phi(\mathbf{r}) = \frac{1}{\varepsilon} \iiint_V d\mathbf{r}' \varrho(\mathbf{r}') \frac{e^{-j\beta|\mathbf{r}-\mathbf{r}'|}}{4\pi|\mathbf{r}-\mathbf{r}'|} \tag{26.1.2}$$

[1]This topic is found in many standard textbooks in electromagnetics [32, 47, 54]. They are also found in lecture notes [44, 139].

where $\beta = \omega\sqrt{\mu\varepsilon} = \omega/c$ is the wavenumber. The integrals in (26.1.1) and (26.1.2) are normally untenable, but when the observation point is far from the source, approximation to the integrals can be made giving them a nice physical interpretation.

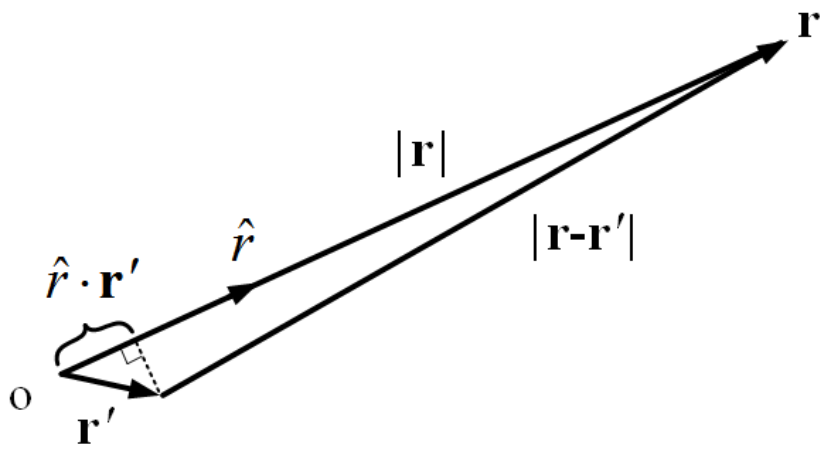

Figure 26.3: The relation between $|\mathbf{r}|$ and $|\mathbf{r}-\mathbf{r}'|$ using the parallax method, or that $|\mathbf{r}-\mathbf{r}'| \approx |\mathbf{r}| - \mathbf{r}' \cdot \hat{r}$. It is assumed that $\mathbf{r}$ is almost parallel to $\mathbf{r} - \mathbf{r}'$.

26.1.1 Far-Field Approximation

When $|\mathbf{r}| \gg |\mathbf{r}'|$, then $|\mathbf{r} - \mathbf{r}'| \approx r - \mathbf{r}' \cdot \hat{r}$, where $r = |\mathbf{r}|$. This approximation can be shown algebraically or by geometrical argument as shown in Figure 26.3. Thus (26.1.1) above becomes

$$\mathbf{A}(\mathbf{r}) \approx \frac{\mu}{4\pi} \iiint_V d\mathbf{r}' \frac{\mathbf{J}(\mathbf{r}')}{r - \mathbf{r}' \cdot \hat{r}} e^{-j\beta r + j\beta \mathbf{r}' \cdot \hat{r}} \approx \frac{\mu e^{-j\beta r}}{4\pi r} \iiint_V d\mathbf{r}' \mathbf{J}(\mathbf{r}') e^{j\beta \mathbf{r}' \cdot \hat{r}} \tag{26.1.3}$$

In the above, $\mathbf{r}' \cdot \hat{r}$ is small compared to r. Hence, we have made use of that $1/(1-\Delta) \approx 1$ when Δ is small, so that $1/(r - \mathbf{r}' \cdot \hat{r})$ can be approximate by $1/r$. Also, we assume that the frequency is sufficiently high such that $\beta \mathbf{r}' \cdot \hat{r}$ is not necessarily small. Thus, $e^{j\beta \mathbf{r}' \cdot \hat{r}} \neq 1$, unless $\beta \mathbf{r}' \cdot \hat{r} \ll 1$. Hence, we keep the exponential term in (26.1.3) but simplify the denominator to arrive at the last expression above.

If we let $\boldsymbol{\beta} = \beta \hat{r}$, which is the $\boldsymbol{\beta}$ vector (or $\mathbf{k}$ vector in optics), and $\mathbf{r}' = \hat{x}x' + \hat{y}y' + \hat{z}z'$, then

$$e^{j\beta \mathbf{r}' \cdot \hat{r}} = e^{j\boldsymbol{\beta} \cdot \mathbf{r}'} = e^{j\beta_x x' + j\beta_y y' + j\beta_z z'} \tag{26.1.4}$$

Therefore (26.1.3) resembles a 3D Fourier transform integral,[2] namely, the above integral

[2]Except that the vector $\boldsymbol{\beta}$ is of fixed length.

becomes

$$\mathbf{A}(\mathbf{r}) \approx \frac{\mu e^{-j\beta r}}{4\pi r} \iiint_V d\mathbf{r}' \mathbf{J}(\mathbf{r}') e^{j\boldsymbol{\beta}\cdot\mathbf{r}'} \tag{26.1.5}$$

and (26.1.5) can be rewritten as

$$\mathbf{A}(\mathbf{r}) \cong \frac{\mu e^{-j\beta r}}{4\pi r} \mathbf{F}(\boldsymbol{\beta}) \tag{26.1.6}$$

where

$$\mathbf{F}(\boldsymbol{\beta}) = \iiint_V d\mathbf{r}' \mathbf{J}(\mathbf{r}') e^{j\boldsymbol{\beta}\cdot\mathbf{r}'} \tag{26.1.7}$$

is the 3D Fourier transform of $\mathbf{J}(\mathbf{r}')$ with the Fourier transform variable $\boldsymbol{\beta} = \hat{r}\beta$.

It is to be noted that this is not a normal 3D Fourier transform because $|\boldsymbol{\beta}|^2 = {\beta_x}^2 + {\beta_y}^2 + {\beta_z}^2 = \beta^2$ which is a constant for a fixed frequency. In other words, the length of the vector $\boldsymbol{\beta}$ is fixed to be β, whereas in a normal 3D Fourier transform, β_x, β_y, and β_z are independent variables, each with values in the range $[-\infty, \infty]$. Or the value of ${\beta_x}^2 + {\beta_y}^2 + {\beta_z}^2$ ranges from zero to infinity.

The above is the 3D "Fourier transform" of the current source $\mathbf{J}(\mathbf{r}')$ with Fourier variables, β_x, β_y, β_z restricted to lying on a sphere of radius β and $\boldsymbol{\beta} = \beta\hat{r}$. This spherical surface in the Fourier space is also called the Ewald sphere.

26.1.2 Locally Plane Wave Approximation

We can write $\hat{r}$ or $\boldsymbol{\beta}$ in terms of direction cosines in spherical coordinates or that

$$\hat{r} = \hat{x}\cos\phi\sin\theta + \hat{y}\sin\phi\sin\theta + \hat{z}\cos\theta \tag{26.1.8}$$

Hence,

$$\mathbf{F}(\boldsymbol{\beta}) = \mathbf{F}(\beta\hat{r}) = \mathbf{F}(\beta, \theta, \phi) \tag{26.1.9}$$

It is not truly a 3D function, since β, the length of the vector $\boldsymbol{\beta}$, is fixed. It is a 3D Fourier transform with data restricted on a spherical surface.

Also in (26.1.6), when $r \gg \mathbf{r}' \cdot \hat{r}$, and when the frequency is high or β is large, $e^{-j\beta r}$ is now a rapidly varying function of r while, $\mathbf{F}(\boldsymbol{\beta})$ is only a slowly varying function of $\hat{r}$ or of θ and ϕ, the observation angles. In other words, the prefactor in (26.1.6), $\exp(-j\beta r)/r$, can be thought of as resembling a spherical wave. Hence, if one follows a ray of this spherical wave and moves in the r direction, the predominant variation of the field is due to $e^{-j\beta r}$, whereas the direction of the vector $\boldsymbol{\beta}$ changes little, and hence, $\mathbf{F}(\boldsymbol{\beta})$ changes little. Furthermore, $\mathbf{r}'$ in (26.1.7) are restricted to small or finite number, making $\mathbf{F}(\boldsymbol{\beta})$ a weak function of $\boldsymbol{\beta}$ (see Figure 26.4).

The above shows that in the far field, the wave radiated by a finite source resembles a spherical wave. Moreover, a spherical wave resembles a plane wave when one is sufficiently far from the source such that $\beta r \gg 1$, or $2\pi r/\lambda \gg 1$. Or r is many wavelengths away from

the source. Hence, we can write $e^{-j\beta r} = e^{-j\boldsymbol{\beta}\cdot\mathbf{r}}$ where $\boldsymbol{\beta} = \hat{r}\beta$ and $\mathbf{r} = \hat{r}r$ so that a spherical wave resembles a plane wave locally. This phenomenon is shown in Figure 26.4 and Figure 26.5

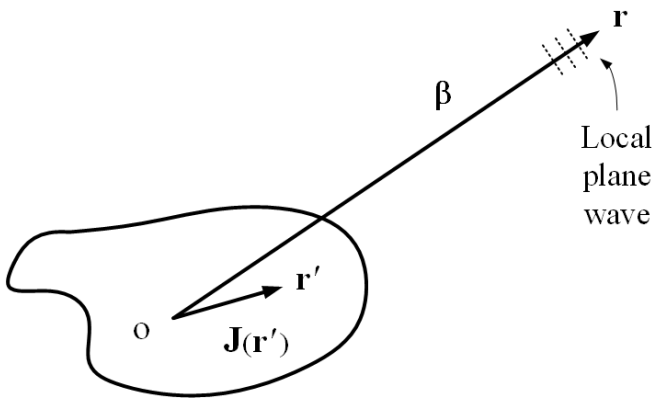

Figure 26.4: A source radiates a field that resembles a spherical wave. In the vicinity of the observation point $\mathbf{r}$, when β is large, the field is strongly dependent on r via $\exp(-j\beta r)$ but weakly dependent on $\boldsymbol{\beta}$ (***b**eta* hardly changes direction in the vicinity of the observation point). Hence, the field becomes locally a plane wave in the far field.

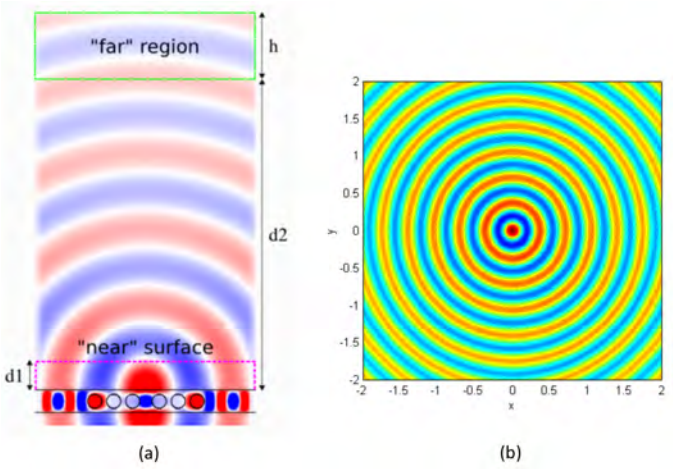

Figure 26.5: (a) A leaky hole in a waveguide leaks a spherical (courtesy of MEEP, MIT). (b) A point source radiates a spherical wave (courtesy of ME513, Purdue Engineering). Most of these simulations are done with FDTD (finite-difference time-domain) method that we will learn later in the course. When the wavelength is short, or the frequency high, a spherical wave front looks locally plane. This is similar to the notion that as humans, who are short, think that the earth is flat around us. Up to this day, some people still believe that the earth is flat:)

Then, it is clear that with the local plane-wave approximation, $\nabla \to -j\boldsymbol{\beta} = -j\beta\hat{r}$, we have

$$\mathbf{H} = \frac{1}{\mu}\nabla \times \mathbf{A} \approx -j\frac{\beta}{\mu}\hat{r} \times (\hat{\theta}A_\theta + \hat{\phi}A_\phi) = j\frac{\beta}{\mu}(\hat{\theta}A_\phi - \hat{\phi}A_\theta) \tag{26.1.10}$$

Similarly [44, 139],

$$\mathbf{E} = \frac{1}{j\omega\varepsilon}\nabla \times \mathbf{H} \cong -j\frac{\beta}{\omega\epsilon}\hat{r} \times \mathbf{H} \cong -j\omega(\hat{\theta}A_\theta + \hat{\phi}A_\phi) \tag{26.1.11}$$

Notice that $\boldsymbol{\beta} = \beta\hat{r}$, the direction of propagation of the local plane wave, is orthogonal to $\mathbf{E}$ and $\mathbf{H}$ in the far field, a property of a plane wave since the wave is locally a plane wave.

Moreover, there are more than one way to derive the electric field $\mathbf{E}$. For instance, using (26.1.10) for the magnetic field, the electric field can also be written as

$$\mathbf{E} = \frac{1}{j\omega\mu\varepsilon}\nabla \times \nabla \times \mathbf{A} \tag{26.1.12}$$

Using the formula for the double-curl operator, the above can be rewritten as

$$\mathbf{E} = \frac{1}{j\omega\mu\varepsilon}\left(\nabla\nabla \cdot \mathbf{A} - \nabla^2\mathbf{A}\right) \cong \frac{1}{j\omega\mu\varepsilon}\left(-\boldsymbol{\beta}\boldsymbol{\beta} + \beta^2\bar{\mathbf{I}}\right) \cdot \mathbf{A} \tag{26.1.13}$$

where we have used that $\nabla \cong -j\boldsymbol{\beta}$ and $\nabla^2\mathbf{A} = -\beta^2\mathbf{A}$.[3] Alternatively, we can factor $\beta^2 = \omega^2\mu\epsilon$ out of the parenthesis, and rewrite the above as

$$\mathbf{E} \cong -j\omega\left(-\hat{\beta}\hat{\beta} + \bar{\mathbf{I}}\right)\cdot\mathbf{A} = -j\omega\left(-\hat{r}\hat{r} + \bar{\mathbf{I}}\right)\cdot\mathbf{A} \tag{26.1.14}$$

Since $\bar{\mathbf{I}} = \hat{r}\hat{r} + \hat{\theta}\hat{\theta} + \hat{\phi}\hat{\phi}$, then the above becomes

$$\mathbf{E} \cong -j\omega\left(\hat{\theta}\hat{\theta} + \hat{\phi}\hat{\phi}\right)\cdot\mathbf{A} = -j\omega(\hat{\theta}A_\theta + \hat{\phi}A_\phi) \tag{26.1.15}$$

which is the same as previously derived. It also shows that the electric field is transverse to the $\boldsymbol{\beta}$ vector.[4]

Furthermore, it can be shown that in the far field, using the local plane-wave approximation,

$$|\mathbf{E}|/|\mathbf{H}| \approx \eta \tag{26.1.16}$$

where η is the intrinsic impedance of free space, which is a property of a plane wave. Moreover, one can show that the time average Poynting's vector, or the power density flow, in the far field is

$$\langle\mathbf{S}\rangle = \frac{1}{2}\Re e\left(\mathbf{E}\times\mathbf{H}^*\right) \approx \frac{1}{2\eta}|\mathbf{E}|^2\hat{r} = \langle S_r\rangle\hat{r} \tag{26.1.17}$$

which resembles also the property of a plane wave.[5] Since the radiated field is a spherical wave, the Poynting's vector is radial. Therefore,

$$\langle\mathbf{S}\rangle = \hat{r}\langle S_r(\theta,\phi)\rangle, \quad \text{where} \quad \langle S_r(\theta,\phi)\rangle = \frac{1}{2\eta}|\mathbf{E}|^2 \tag{26.1.18}$$

and $\langle S_r\rangle$ is the time-average radial power density. The plot of $|\mathbf{E}(\theta,\phi)|$ is termed the far-field pattern or the radiation pattern of an antenna or the source, while the plot of $|\mathbf{E}(\theta,\phi)|^2$ is its far-field power pattern.

26.1.3 Directive Gain Pattern Revisited

We have defined the directive gain pattern for a Hertzian dipole before in Section 25.3. But this concept can be applied to a general radiating source or antenna. Once the far-field radiation power pattern or the radial power density $\langle S_r\rangle$ is known, the total power radiated by the antenna in the far field can be found by integrating over all angles, viz.,

$$P_T = \int_0^\pi \int_0^{2\pi} r^2 \sin\theta d\theta d\phi \langle S_r(\theta,\phi)\rangle \tag{26.1.19}$$

[3]Note that $\nabla\cdot\mathbf{A} \neq 0$ here.

[4]We can also arrive at the above by letting $\mathbf{E} = -j\omega\mathbf{A} - \nabla\Phi$, and using the appropriate formula for the scalar potential. There is more than one road that lead to Rome!

[5]To avoid confusion, we will use $\mathbf{S}$ to denote instantaneous Poynting's vector and $\underline{\mathbf{S}}$ to denote complex Poynting's vector (see 10.3.1).

The above evaluates to a constant independent of r due to energy conservation. Now assume that this same antenna is radiating isotropically in all directions, then the average power density of this fictitious isotropic radiator as $r \to \infty$ is

$$\langle S_{\text{av}} \rangle = \frac{P_T}{4\pi r^2} \tag{26.1.20}$$

A dimensionless directive gain pattern can be defined as before in Section 25.3 such that [32, 139]

$$G(\theta, \phi) = \frac{\langle S_r(\theta, \phi) \rangle}{\langle S_{\text{av}} \rangle} = \frac{4\pi r^2 \langle S_r(\theta, \phi) \rangle}{P_T} \tag{26.1.21}$$

This directive gain pattern is a measure of the radiation power pattern of the antenna or source compared to when it radiates isotropically. The above function is independent of r in the far field since $S_r \sim 1/r^2$ in the far field. As in the Hertzian dipole case, the directivity of an antenna $D = \max(G(\theta, \phi))$, is the maximum value of the directive gain. It is to be noted that by its mere definition,

$$\int d\Omega G(\theta, \phi) = 4\pi \tag{26.1.22}$$

where $\int d\Omega = \int_0^{2\pi} \int_0^{\pi} \sin\theta d\theta d\phi$. It is seen that since the directive gain pattern is normalized, when the radiation power is directed to the main lobe of the antenna, the corresponding side lobes and back lobes will be diminished.

An antenna also has an effective area or aperture A_e, such that if a plane wave carrying power density denoted by $\langle S_{\text{inc}} \rangle$ impinges on the antenna, then the power received by the antenna, P_{received} is given by

$$P_{\text{received}} = \langle S_{\text{inc}} \rangle A_e \tag{26.1.23}$$

Here, the transmit antenna and the receive antenna are in the far field of each other. Hence, we can approximate the field from the transmit antenna to be a plane wave when it reaches the receive antenna. If the receive antenna is made of PEC, induced current will form on the receive antenna so as to generated a field that will cancel the incident field on the PEC surface. This induced current generates a voltage at the receiver load, and hence power received by the antenna.

A wonderful relationship exists between the directive gain pattern $G(\theta, \phi)$ and the effective aperture, namely that[6]

$$A_e = \frac{\lambda^2}{4\pi} G(\theta, \phi) \tag{26.1.24}$$

Therefore, the effective aperture of an antenna is also direction dependent. The above implies that the radiation property of an antenna is related to its receiving property. This is a

[6]The proof of this formula is beyond the scope of this lecture, but we will elaborate on it when we discuss reciprocity theorem.

beautiful consequence of reciprocity theorem that we will study later! The constant of proportionality, $\lambda^2/(4\pi)$ is a universal constant that is valid for all antennas satisfying reciprocity theorem. The derivation of this constant for a Hertzian dipole is given in Kong [32], or using blackbody radiation law [139, 140].

The directivity and the effective aperture can be enhanced by designing antennas with different gain patterns. When the radiative power of the antenna can be directed to be in a certain direction, then the directive gain and the effective aperture (for that given direction) of the antenna is improved. This is shown in Figure 26.6. Such focussing of the radiation fields of the antenna can be achieved using reflector antennas or array antennas. Array antennas, as shall be shown, work by constructive and destructive wave field of the antenna.

Being able to do point-to-point communications at high data rate is an important modern application of antenna array. Figure 26.7 shows the gain pattern of a sophisticated antenna array design for 5G applications.

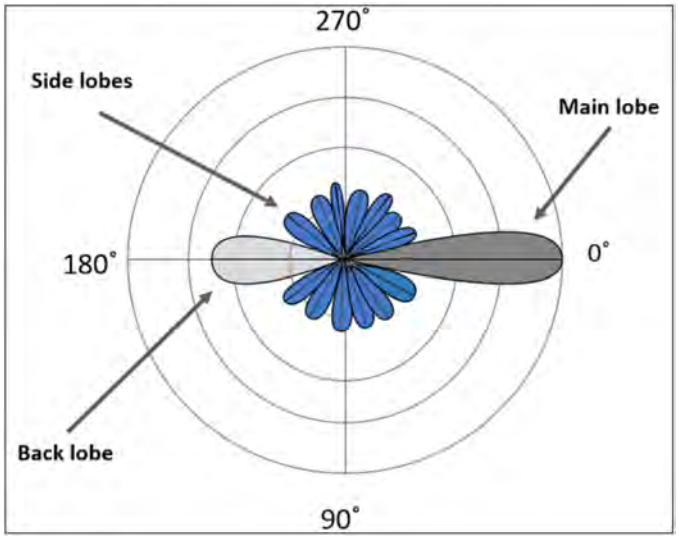

Figure 26.6: The directive gain pattern of an array antenna. The directivity is increased by constructive interference (courtesy of Wikepedia).

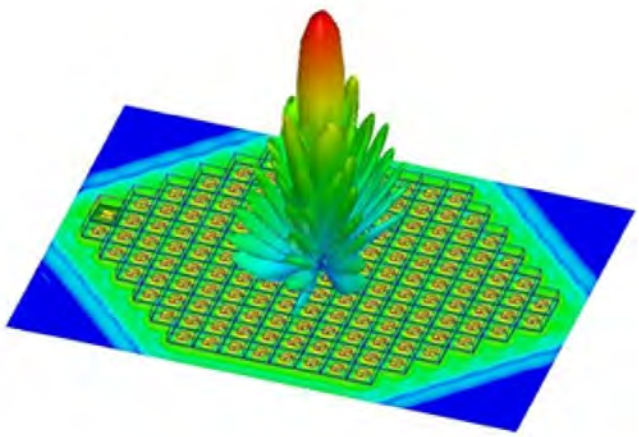

Figure 26.7: The directive gain pattern of a sophisticated array antenna for 5G applications (courtesy of Ozeninc.com).